

# Rich spatial–temporal dynamics in a diffusive population model for pioneer–climax species

Ying Su · Xingfu Zou

Received: 4 July 2017 / Accepted: 10 November 2018 / Published online: 19 November 2018  
© Springer Nature B.V. 2018

**Abstract** A general diffusive population model for interactions of pioneer and climax species subject to the no-flux boundary condition is considered. Local and global steady-state bifurcations as well as Hopf bifurcations are investigated. A condition for Turing instability not to happen is obtained, and the conditions for occurrences of Turing bifurcations and Hopf bifurcations are also obtained. Numerical simulations are carried out to demonstrate and extend the obtained analytic results which suggest that the spatial diffusion may make the climax species more dominant. The results indicate that the model, with spatial diffusion incorporated, can have very rich spatial–temporal dynamics.

**Keywords** Pioneer species · Climax species · Diffusion · Hopf bifurcation · Turing bifurcation · Spatial–temporal pattern

Research supported by the Natural Science and Engineering Council of Canada (Grant No. RGPIN-2016-04665), National Natural Science Foundation of China (No: 11201096, 11461024) and the Fundamental Research Funds for the Central Universities and Program for Innovation Research of Science in Harbin Institute of Technology.

Y. Su  
Department of Mathematics, Harbin Institute of  
Technology, Harbin 150001, Heilongjiang,  
People's Republic of China  
e-mail: ysu@hit.edu.cn

X. Zou (✉)  
Department of Applied Mathematics, University of  
Western Ontario, London, ON N6A 5B7, Canada  
e-mail: xzou@uwo.ca

**Mathematics Subject Classification** 35B32 · 35K57 · 92B05 · 92D25

## 1 Introduction

Population growth of a single species is often modeled by  $u' = uh(u)$ , where the fitness function  $h$  is chosen according to some basic characteristics of the species under consideration. To model a pioneer species that flourishes at very small population densities but progressively do worse as densities increase due to the crowding effect, Verhulst [23] and Ricker [15] chose a decreasing fitness function allowing a unique zero, which is similar to  $f$  illustrated in Fig. 1. To model a climax species that requires a minimum threshold for survival, flourishes at appropriately higher population densities due to the benefits of group defense or other aggregate behaviors, and yet, struggles/suffers at further higher densities due to overcrowding effect, Allee [1] choose another function that has the properties of the function  $g$  as shown in Fig. 1.

To study the interaction of a pioneer and a climax species, Selgrade and Namkoong [17] proposed the following model:

$$\begin{cases} u' = uf(c_{11}u + c_{12}v), \\ v' = vg(c_{21}u + c_{22}v), \end{cases} \quad (1.1)$$

where  $u$  and  $v$  represent the populations of the pioneer and climax species, respectively,  $f$  and  $g$  are the pio-

neer and climax fitness functions, respectively, which are assumed to be dependent on the weighted total population of both species. Here,  $c_{ij} > 0$  ( $i, j = 1, 2$ ) reflect the interaction strengths of species  $j$  on the species  $i$ . By the nature of climax and pioneer species,  $f$  and  $g$  satisfy the following general assumptions:

$$f'(z_1) < 0 \text{ and } f(z_1) = 0, \quad (1.2)$$

$$g \in C^1 \text{ has exact two zeros: } 0 < z_2^+ < z_2^- \text{ and } g'(z_2^-) < 0 < g'(z_2^+). \quad (1.3)$$

Under (1.2) and (1.3), system (1.1) can have various structures of equilibria, depending on the amplitudes of the three positive numbers  $z_1$ ,  $z_2^-$  and  $z_2^+$  (see Fig. 1) which are determined by particular forms of functions  $f$  and  $g$  and the parameters therein.

In (1.1), there are four weight parameters, but after a rescaling, we only need to consider two parameters, as in the following scaled system

$$\begin{cases} u' = uf(c_1u + v), \\ v' = vg(u + c_2v). \end{cases} \quad (1.4)$$

As was shown in [3], when  $c_1 \neq z_1/z_2^\pm$  and  $c_2 \neq z_2^\pm/z_1$ , the equilibria as well as their local stability for (1.4) can be described by Fig. 2, where the “•” denotes the stable equilibrium, “o” denotes the unstable equilibrium and “\*” denotes the equilibrium whose stability further depends on the values of parameters  $c_1$  and  $c_2$ . We refer to [3, 18, 21] for the qualitative study of long-term behaviors including the stability of the equilibria and Hopf bifurcations.

It is well known that spatial effect is an important factor in ecology, and it is indeed considered as one of the major factors that contribute to biological diversity in the real world. Moreover, in the presence of spatial effects, diffusion can have a complicated impacts on spatial ecology. For example, incorporating diffusion into a reaction (or kinetic) system, the diffusion destroys the stability of an equilibrium (Turing instability) leading to the formation of certain patterns (see, e.g., [22], or [5]) and the rich references therein), or drive a temporally periodic but spatially homogeneous dynamics to a spatially heterogeneous oscillation (see, e.g., [20]); the diffusion can also drive the solution to blow-up at finite time (see, e.g., [11]), or drive an otherwise persistent competing species to extinction (see, e.g., [6]). There are also diffusive models which can preserve the dynamics of the corresponding ODE mod-

els. In other worlds, it all depends on the nonlinearity/nonlinearities in the reaction equation(s) and their interplay with the diffusion, and hence, for any given reaction diffusion model system, its spatial-temporal dynamics needs to be analyzed separately.

Adding spatial and random movement (diffusion) into (1.4) results in the following reaction-diffusion model

$$\begin{cases} \frac{\partial u}{\partial t} = d_1 \frac{\partial^2 u}{\partial x^2} + uf(c_1u + v), \\ \frac{\partial v}{\partial t} = d_2 \frac{\partial^2 v}{\partial x^2} + vg(u + c_2v), \end{cases} \quad (1.5)$$

which has recently been investigated under some scenarios for the habitat domain with different boundary conditions. In the case of bounded habitat domain, Buchanan [4] gave a sufficient condition for the Turing instability to happen under no-flux boundary condition, and Liu and Wei [10] investigated Hopf bifurcation under the zero Dirichlet boundary condition. Assuming the habitat is the whole spatial space, Brown et. al. [2], Yuan and Zou [27] and Weng and Zou [25] explored the existence of traveling wave fronts and spreading speeds when the interaction coefficients are in certain ranges.

In both cases of bounded and unbounded domains, understanding the solutions dynamics of (1.5) is far from complete, and there are wide parameter ranges for which the dynamics remains unclear. The goal of this paper is to further explore system (1.5) subject to the no-flux boundary condition in an bounded domain, with emphasis on the spatial-temporal dynamics and the effect of the diffusion on the dynamics. That is, we will study the following boundary value problem

$$\begin{cases} \frac{\partial u}{\partial t} = \frac{\partial^2 u}{\partial x^2} + uf(c_1u + v), \text{ in } (0, +\infty) \times \Omega, \\ \frac{\partial v}{\partial t} = d \frac{\partial^2 v}{\partial x^2} + vg(u + c_2v), \text{ in } (0, +\infty) \times \Omega, \\ \frac{\partial u(t,0)}{\partial x} = \frac{\partial u(t,\pi)}{\partial x} = 0, \text{ on } (0, +\infty) \times \partial\Omega. \end{cases} \quad (1.6)$$

Here, for simplicity, we will consider the simplest bounded domain  $\Omega = (0, \pi)$ . We will study the dynamics of (1.6), by comparing with the dynamics of (1.4), which can be considered as a subsystem of (1.6), and we hope to gain some insights on the impact the spatial diffusion on the spatial-temporal dynamics.

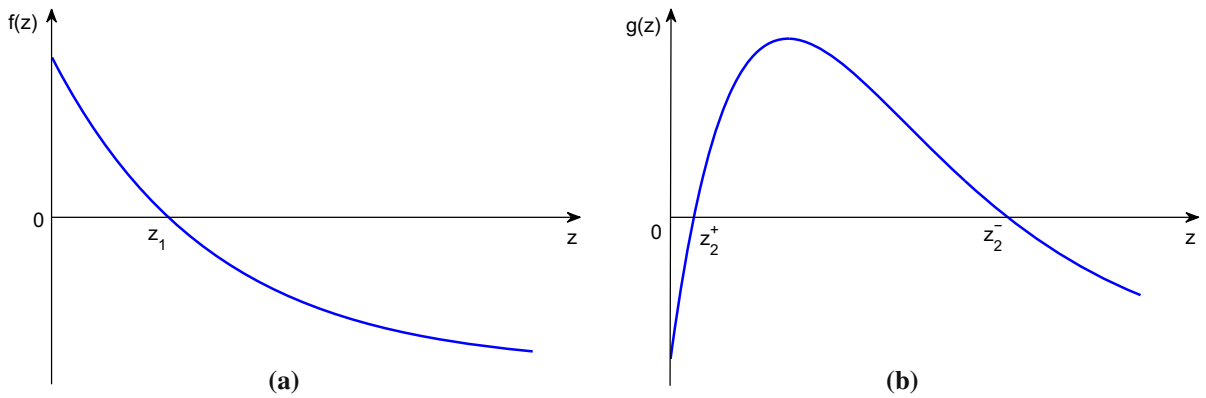


**Fig. 1** Diagrams of fitness functions for pioneer (a) and climax (b) species

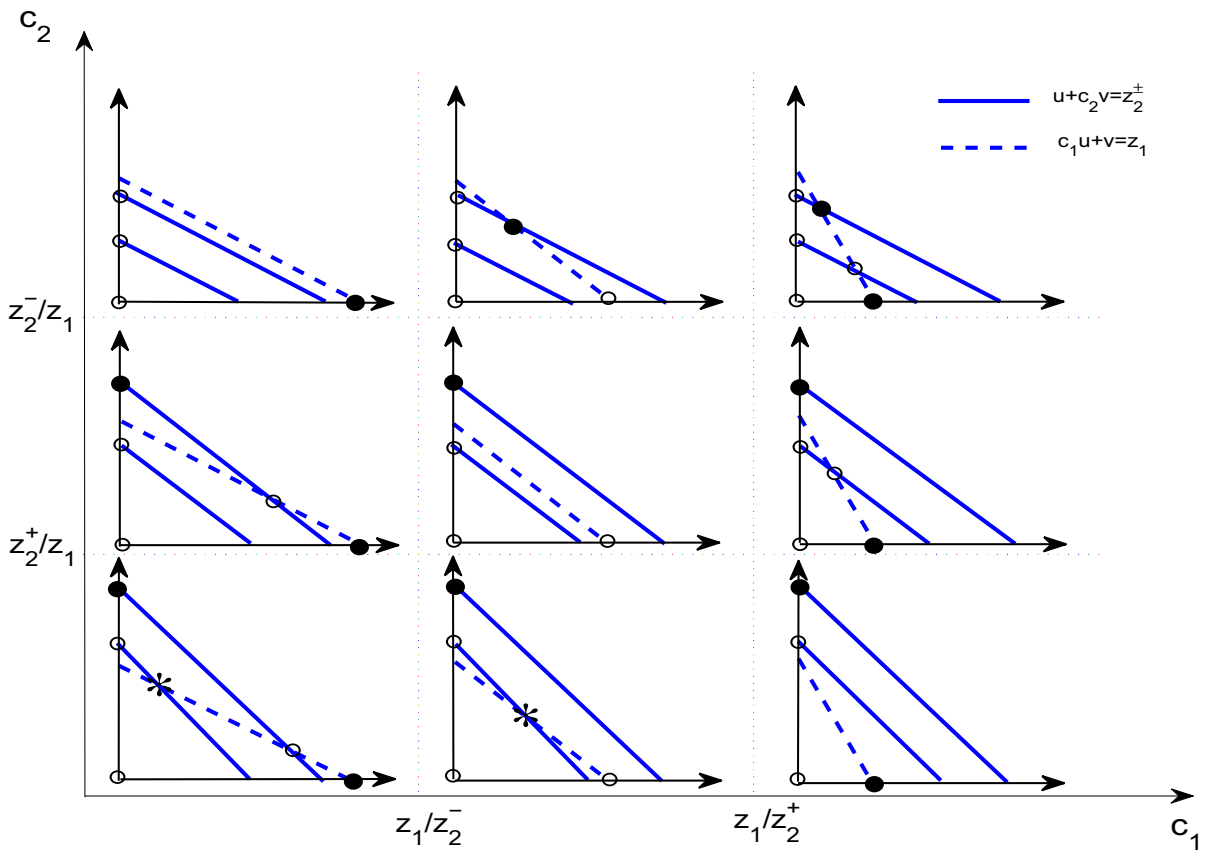


**Fig. 2** Structure of equilibria and their stability for the non-spatial model (1.4), depending on the ranges of the parameters  $c_1$  and  $c_2$

In what follows, we always assume that  $c_1 \neq z_1/z_2^\pm$  and  $c_2 \neq z_2^\pm/z_1$  to exclude the critical cases. Due to the no-flux boundary condition, systems (1.6) and (1.4) share the same constant steady states. We show that the linear stability of all constant *boundary* steady states for

(1.6) are the same as for (1.4) and the linearly *unstable constant coexistence steady states* of (1.4) still remain linearly unstable in (1.6). All these suggests that we only need to focus on the interior positive constant steady states, and we choose  $(u^*, v^*)$  labeled by “\*”

in Fig. 2 to work on. We derive a very simple sufficient condition, that is,  $d \geq z_2^+ g'(z_2^+)$ , for the Turing bifurcation not to occur, and this condition greatly improves the corresponding condition  $d \geq \hat{d}$  in [4] where  $\hat{d}$  may tend to  $\infty$  by varying  $c_2$ . We then further investigate, vigorously and with details, the local/global steady-state bifurcation and Hopf bifurcation near this constant steady state. Using  $c_2$  as the bifurcation parameter, the numerical results suggest that the bifurcated steady states branch connects to the climax boundary equilibrium. These results indicate that the model, after incorporated with spatial diffusion, can allow very rich spatial–temporal dynamics/patterns, revealing the impact that the spatial diffusion can have.

We point out that by using the same approach, spatial–temporal dynamics/patterns have also been recently explored for some other model systems, see, e.g., [8,9,14,24,28,29]. However, the rich structure of constant steady states of (1.6), corresponding to the various positions of the *three* lines in Fig. 2, allows various parameter ranges that would lead to different natures of the interactions between the two species. As such, it is worthwhile and important to investigate the spatial–temporal dynamics/patterns of (1.6) with various scenarios of the constant steady states of this model.

The rest of this paper is organized as follows: In the next section, we establish the well posedness of initial value problem of (1.6) and study the linear stability of constant steady states. In Sect. 3, we investigate the steady-state and Hopf bifurcations. Finally, we conduct some numerical simulations to illustrate and extend the analytic results.

## 2 Well posedness and linear stability

In this section, we first establish the well posedness of the initial value problem of (1.6), and then, we prove that the constant steady states labeled by “•” and “○” in Fig. 2 have the same linear stability/instability for system (1.6) as for (1.4).

**Lemma 2.1** *For any given nonnegative initial function  $(u_0, v_0) \in C([0, \pi], \mathbb{R}^2)$ , (1.6) admits a unique nonnegative bounded solution defined for all  $t \in (0, \infty)$ .*

*Proof* The local existence and uniqueness of solutions follows from the standard results of parabolic equations [7]. Let  $[0, T_0)$  be the maximal interval of exist-

tence, where  $T_0$  is  $+\infty$  if the solution is bounded in  $t \in [0, T_0)$ . Let  $\gamma := f(0) = \max_{z \in \mathbb{R}} f(z)$  and  $U(t, x) := e^{-\gamma t} u(t, x)$ . Then,  $U(t, x)$  satisfies

$$\begin{cases} \frac{\partial U(t,x)}{\partial t} = \frac{\partial^2 U(t,x)}{\partial x^2} - U(t,x)[\gamma - f(c_1 u(t,x) + v(t,x))], \\ \frac{\partial U(t,0)}{\partial x} = \frac{\partial U(t,\pi)}{\partial x} = 0, \\ U(0,x) \geq 0. \end{cases}$$

Using [12, Lemma 4.1, page 19] we obtain that  $U(t, x) \geq 0$  for all  $t \in [0, T_0)$  because  $\gamma - f(c_1 u(t, x) + v(t, x)) \geq 0$ . It then follows that  $u(t, x) \geq 0$  for all  $t \in [0, T_0)$ . Similarly, we can obtain that  $v(t, x) \geq 0$  for all  $t \in [0, T_0)$ . Let  $M_1 := \max_{x \in [0, \pi]} u_0(x)$ , and  $z(t)$  be the solution to the following problem

$$\begin{cases} \frac{dz}{dt} = f(c_1 z), \\ z(0) = M_1. \end{cases}$$

Then, from the monotonicity of  $f$  and the comparison principle we have  $u(t, x) \leq z(t)$  for all  $t \in [0, T_0)$  and  $x \in [0, \pi]$ . Note that  $\lim_{t \rightarrow +\infty} z(t) = z_1/c_1$ , it follows that  $u(t, x)$  is bounded in  $t \in [0, T_0)$ . On the other hand, let  $M_2 = \max\{\max_{x \in [0, \pi]} v(0, x), \max_{z \in \mathbb{R}} g(z)\}$ , then it is not difficult to obtain that  $v(t, x) \leq M_2$  for  $t \in [0, T_0)$  by using the comparison principle. Thus,  $T_0 = +\infty$  and the solution is nonnegative and bounded.  $\square$

Define  $X := \{(u, v) \in H^2(0, \pi) \times H^2(0, \pi), u'(0) = u'(\pi) = v'(0) = v'(\pi) = 0\}$  and  $\mathbb{N}_0 := \{0\} \cup \mathbb{N}$ , where  $\mathbb{N}$  is the set of natural number. Linearizing system (1.6) at a constant steady state  $(u_e, v_e)$  yields

$$\frac{\partial}{\partial t} \begin{pmatrix} u \\ v \end{pmatrix} = L \begin{pmatrix} u \\ v \end{pmatrix},$$

where the operator  $L : X \rightarrow X$  is defined by

$$L := \begin{pmatrix} \frac{\partial^2}{\partial x^2} + A & B \\ C & d \frac{\partial^2}{\partial x^2} + D \end{pmatrix}, \tag{2.1}$$

with

$$\begin{aligned} A &= f(c_1 u_e + v_e) + c_1 u_e f'(c_1 u_e + v_e), \\ B &= u_e f'(c_1 u_e + v_e), \\ C &= v_e g'(u_e + c_2 v_e), \\ D &= g(u_e + c_2 v_e) + c_2 v_e g'(u_e + c_2 v_e). \end{aligned}$$

Note that the eigenvalue problem

$$\varphi''(x) = \lambda\varphi(x), \quad \varphi'(0) = \varphi'(\pi) = 0,$$

has eigenvalues  $-n^2$ ,  $n \in \mathbb{N}_0$  with corresponding eigenfunctions  $\cos(nx)$ , which forms an orthonormal basis of the space  $\mathcal{L}^2(0, \pi)$ . Next we look for eigenfunctions of  $L$  in  $X$ . For this purpose, we assume that

$$\begin{pmatrix} \phi \\ \psi \end{pmatrix} = \sum_{n=0}^{\infty} \cos(nx) \begin{pmatrix} a_n \\ b_n \end{pmatrix}$$

is an eigenfunction of  $L$  with the corresponding eigenvalue  $\lambda$ . Then, by a straightforward analysis, we conclude that there exists  $n \in \mathbb{N}_0$  such that

$$L_n \begin{pmatrix} a_n \\ b_n \end{pmatrix} = \lambda \begin{pmatrix} a_n \\ b_n \end{pmatrix}, \tag{2.2}$$

where

$$L_n := \begin{pmatrix} -n^2 + A & B \\ C & -dn^2 + D \end{pmatrix}. \tag{2.3}$$

Let  $\text{tr}(L_n)$  and  $\det(L_n)$  be the trace and determinant of the matrix  $L_n$ , respectively. Denote

$$\Delta_n(\lambda) := \lambda^2 - \text{tr}(L_n)\lambda + \det(L_n), \quad n \in \mathbb{N}_0. \tag{2.4}$$

It then follows that  $\lambda$  is a eigenvalue of  $L$  if and only if there exists  $n \in \mathbb{N}_0$  such that  $\Delta_n(\lambda) = 0$ , and the corresponding eigenfunction is  $\cos(nx)(a_n, b_n)^T$ . We call  $\Delta_n(\lambda) = 0$  the  $n$ -th branch of the characteristic equation. Since the sign of the real part of  $\lambda$  determines the linear stability, it suffices to study the quantities  $\text{tr}(L_n)$  and  $\det(L_n)$ .

Now we are in the position to present the stability/instability of steady states of (1.6). It turns out that diffusion does not change the stability of the constant steady states labeled by “•” and “o” in Fig. 2. We note that the nine sub-figures are organized in terms of the values of  $c_1$  and  $c_2$ .

**Lemma 2.2** *The following statements hold.*

- (i) All steady states labeled by “o” in Fig. 2 are linearly unstable.
- (ii) All steady states labeled by “•” in Fig. 2 are linearly stable.

*Proof* For (i), since a the steady state of (1.4) labeled by “o” has an unstable manifold in  $\mathbb{R}^2$  and (1.4) is a subsystem of (1.6), “o” also remain linearly unstable as a steady state of (1.6).

For (ii), we first notice that, by their forms of “•” type equilibria, all “•” type belong to the set  $\Sigma = \Sigma_1 \cup \Sigma_2 \cup \Sigma_3$ , where

$$\begin{aligned} \Sigma_1 &= \left\{ \left( 0, \frac{z_2^-}{c_2} \right) : c_2 < \frac{z_2^-}{z_1} \right\} = \{(0, v) : v > z_1\} \\ \Sigma_2 &= \left\{ \left( \frac{z_1}{c_1}, 0 \right) : c_1 < \frac{z_1}{z_2^-} \text{ or } c_1 > \frac{z_1}{z_2^+} \right\} \\ &= \{(u, 0) : u > z_2^- \text{ or } u < z_2^+\} \\ \Sigma_3 &= \left\{ \left( \frac{z_2^- - c_2 z_1}{1 - c_1 c_2}, \frac{z_1 - c_1 z_2^-}{1 - c_1 c_2} \right) : \right. \\ &\quad \left. c_1 > \frac{z_1}{z_2^-} \text{ and } c_2 > \frac{z_2^-}{z_1} \right\} \end{aligned}$$

If  $\bullet \in \Sigma_1$ , then the corresponding quantities

$$\begin{aligned} \text{tr}(L_n) &= -n^2(1 + d) + z_2^- g'(z_2^-) \\ &\quad + f(z_2^-/c_2), \quad n \in \mathbb{N}_0, \\ \det(L_n) &= dn^4 - [df(z_2^-/c_2) + z_2^- g'(z_2^-)]n^2 \\ &\quad + z_2^- f(z_2^-/c_2)g'(z_2^-), \quad n \in \mathbb{N}_0. \end{aligned} \tag{2.5}$$

By a direct calculation, we obtain that  $\lambda_{1n} = -n^2 + f(z_2^-/c_2)$  and  $\lambda_{2n} = -dn^2 + z_2^- g'(z_2^-)$ ,  $n \in \mathbb{N}_0$  are all eigenvalues. Note that  $f(z_2^-/c_2) < 0$  and  $g'(z_2^-) < 0$  due to condition  $c_2 < z_2^-/z_1$ . It follows that the steady state  $(0, z_2^-/c_2)$  is linearly stable. By a similar calculation, we can prove the conclusion when  $\bullet \in \Sigma_2$ .

If  $\bullet \in \Sigma_3$ , then the corresponding quantities

$$\begin{aligned} \text{tr}(L_n) &= -n^2(1 + d) + c_1 u_e f'(z_1) \\ &\quad + c_2 v_e g'(z_2^-), \quad n \in \mathbb{N}_0, \\ \det(L_n) &= dn^4 - [dc_1 u_e f'(z_1) + c_2 v_e g'(z_2^-)]n^2 \\ &\quad - (1 - c_1 c_2) u_e v_e f'(z_1) g'(z_2^-), \quad n \in \mathbb{N}_0. \end{aligned}$$

Since  $c_1 > z_1/z_2^-$  and  $c_2 > z_2^-/z_1$ ,  $f'(z_1) < 0$ ,  $g'(z_2^-) < 0$  and  $1 - c_1 c_2 < 0$ . Therefore,  $\text{tr}(L_n) < 0$  and  $\det(L_n) > 0$  for all  $n \in \mathbb{N}_0$ . It then follows that all eigenvalues have negative real parts. The proof is completed.  $\square$

*Remark 2.3* When  $c_1 > z_1/z_2^-$  and  $c_2 > z_2^-/z_1$ , near the positive steady state  $(u^*, v^*) = (\frac{z_2^- - c_2 z_1}{1 - c_1 c_2}, \frac{z_1 - c_1 z_2^-}{1 - c_1 c_2})$ ,  $f(c_1 u + v)$  is decreasing in  $v$  and  $g(u + c_2 v)$  is

decreasing in  $u$ . This implies that (1.6) is of competitive type interaction near  $(u^*, v^*)$ . In such a case, we may infer from Lemma 2.2-(ii) that no Turing bifurcation can occur. However when  $c_1 < z_1/z_2^+$  and  $c_2 < z_2^+/z_1$ , near the positive steady state  $(u^*, v^*) = (\frac{z_2^+ - c_2 z_1}{1 - c_1 c_2}, \frac{z_1 - c_1 z_2^+}{1 - c_1 c_2})$ ,  $f(c_1 u + v)$  is decreasing in  $v$  and  $g(u + c_2 v)$  is increasing in  $u$ . This implies that (1.6) is of predator-prey type interaction near  $(u^*, v^*)$ . In such a case, Turing bifurcation may occur around  $(u^*, v^*)$ . Lemma 2.2 also implies that there is neither Hopf bifurcation nor steady-state bifurcation near the steady states labeled by “•”.

### 3 Bifurcations

#### 3.1 Steady states bifurcations and Turing instability

All constant steady states labeled by  $\circ$  and  $\bullet$  in Fig. 2 have been studied in the previous section and have been excluded for possible stability switch due to spatial diffusion. In this section, we study the stability/instability of the constant steady states labeled by  $*$  in Fig. 2. This means that we only focus on the case where  $c_1 < z_1/z_2^+$  and  $c_2 < z_2^+/z_1$  and the constant steady state of interest is given by the formula  $(u^*, v^*) = (\frac{z_2^+ - c_2 z_1}{1 - c_1 c_2}, \frac{z_1 - c_1 z_2^+}{1 - c_1 c_2})$ .

As is seen in the proof of Lemma 2.2-(ii), there are two corresponding quantities that determine the linear stability:

$$\begin{aligned} \text{tr}(L_n) &= -n^2(1 + d) + c_1 u^* f'(z_1) \\ &\quad + c_2 v^* g'(z_2^+), \quad n \in \mathbb{N}_0, \\ \det(L_n) &= dn^4 - [dc_1 u^* f'(z_1) + c_2 v^* g'(z_2^+)]n^2 \\ &\quad - (1 - c_1 c_2)u^* v^* f'(z_1)g'(z_2^+), \quad n \in \mathbb{N}_0. \end{aligned}$$

In the sequel, we use  $c_2$  as the parameter and for the sake of convenience we write  $L_n(c_2)$  instead of  $L_n$ . Let  $p = n^2$ , then  $\det(L_n(c_2)) = 0$  reduces to  $h(p) = 0$ , where  $h(p)$  is a quadratic function defined by

$$\begin{aligned} h(p) &= dp^2 - [dc_1 u^* f'(z_1) + c_2 v^* g'(z_2^+)]p \\ &\quad - (1 - c_1 c_2)u^* v^* f'(z_1)g'(z_2^+), \quad p > 0. \end{aligned} \tag{3.1}$$

The existence of zeros of  $h(p)$  plays an important role in the study of bifurcation. It has been shown in [4] that  $h(p)$  has no zero if  $d > \hat{d}$  where

$$\hat{d} = -\frac{v^* g'(z_2^+)}{c_1^2 u^* f'(z_1)} \left(1 + \sqrt{1 - c_1 c_2}\right)^2, \tag{3.2}$$

and hence, no Turing bifurcation can happen under this condition. We point out that by the dependence of  $u^*$  on  $c_2$ , one easily sees that  $\hat{d} \rightarrow \infty$  as there  $c_2 \rightarrow (z_2^+/z_1)^-$ , meaning that  $\hat{d}$  can become arbitrarily large. In the following, we improve this condition to a much weaker one:  $d \geq z_2^+ g'(z_2^+)$ . For this purpose, we first establish a property of the discriminant of  $h(p) = 0$ .

**Lemma 3.1** *Given  $f, g, z_1, z_2^+, d$  and  $c_1$ , the following equation for  $c_2$*

$$\begin{aligned} &(c_1 d u^* f'(z_1) + c_2 v^* g'(z_2^+))^2 \\ &\quad + 4d(1 - c_1 c_2)u^* v^* f'(z_1)g'(z_2^+) = 0. \end{aligned}$$

*admits a solution  $\hat{c}_2 \in (0, z_2^+/z_1)$  such that  $h(p)$  has two positive zeros  $p_+(c_2) \leq p_-(c_2)$  when  $c_2 \in (\hat{c}_2, z_2^+/z_1]$  and it has no zero point when  $c_2 < \hat{c}_2$ . Moreover,  $p_-(c_2)$  is increasing, and  $p_+(c_2)$  is decreasing in  $c_2$ . Besides,  $p_+(\hat{c}_2) = p_-(\hat{c}_2)$ ,  $p_+(z_2^+/z_1) = 0$  and  $p_-(z_2^+/z_1) = z_2^+ g'(z_2^+)/d$ .*

*Proof* Since  $f'(z_1) < 0$  and  $g'(z_2^+) > 0$ , it is not difficult to check that when  $c_2 = 0$ ,  $h(p) > 0$  for all  $p \geq 0$ . When  $c_2 = z_2^+/z_1$ ,  $h(p) = 0$  has two solutions 0 and  $z_2^+ g'(z_2^+)/d$ . For each fixed  $p > 0$ , we calculate to obtain

$$\begin{aligned} &\frac{d}{dc_2} h(p) \\ &= \frac{-p[(z_1 - c_1 z_2^+)g'(z_2^+) - c_1 d(z_1 - c_1 z_2^+)f'(z_1)]}{(1 - c_1 c_2)^2} \\ &\quad + \frac{z_1(z_1 - c_1 z_2^+)f'(z_1)g'(z_2)}{1 - c_1 c_2} \\ &\quad + \frac{c_1(z_1 - c_1 z_2^+)(z_2^+ - c_2 z_1)f'(z_1)g'(z_2)}{1 - c_1 c_2} \\ &< 0, \end{aligned}$$

which means that  $h(p)$  is decreasing in  $c_2$  for all  $p > 0$ . Therefore, there exists  $\hat{c}_2 > 0$  such that  $h(p)$  has no zero point when  $c_2 < \hat{c}_2$  and  $h(p)$  has two zero points  $p_{\pm}(c_2) > 0$  when  $c_2 \in (\hat{c}_2, z_2^+/z_1]$ . Moreover,  $p_+(c_2)$  and  $p_-(c_2)$  are strictly decreasing and increasing in  $c_2$ , respectively. When  $c_2 = \hat{c}_2$ ,  $\min_{p>0} h(p) = 0$  and

$$\begin{aligned} &\frac{(c_1 d u^* f'(z_1) + \hat{c}_2 v^* g'(z_2^+))^2}{4d} \\ &\quad - (1 - c_1 \hat{c}_2)u^* v^* f'(z_1)g'(z_2^+) = 0. \end{aligned}$$

The proof is completed. □

By the bifurcation theory for R-D systems (see, e.g., [26, Theorem 3.2]), steady-state bifurcation can occur

only if there exists a nature number  $n$  such that  $h(n^2) = 0$ . We then immediately obtain a sufficient condition on the diffusion rate to exclude the possibility of steady-state bifurcation, which also immediately leads to a necessary condition for Turing instability to occur.

**Theorem 3.2** *If  $d \geq z_2^+ g'(z_2^+)$ , then there is no steady-state bifurcation for (1.6), and hence, Turing bifurcation can not occur.*

*Proof* By the proof of Lemma 3.1, for  $c_2 \in (0, \hat{c}_2)$ , the equation  $h(p) = 0$  has no real roots; for  $c_2 \in [\hat{c}_2, z_2^+/z_1)$ ,  $h(p) = 0$  has two positive roots  $p_+(c_2)$  and  $p_-(c_2)$   $0 < p_+(c_2) \leq p_-(c_2) < z_2^+ g'(z_2^+)/d$ . Therefore, for  $c_2 \in (0, z_2^+/z_1)$ , either  $h(p) = 0$  has no real roots, or it has real roots but they are less than 1, implying that there is no positive integer  $n$  such  $h(n^2) = 0$ . It follows that no steady-state bifurcation can occur under the condition  $d \geq z_2^+ g'(z_2^+)$ .  $\square$

The above theorem implies that  $d < z_2^+ g'(z_2^+)$  is a necessary condition for steady-state bifurcation which will be assumed in the following. Under this condition, by Lemma 3.1, at least for  $n = 1$ , there is a  $c_2^{S_1} \in (0, z_2^+/z_1)$  such that  $h(1^2) = 0$  when  $c_2 = c_2^{S_1}$ . For general integer  $n \geq 1$ , let  $c_2^{S_n} \in (0, z_2^+/z_1)$  denote the value of  $c_2$ , if any, at which  $h(n^2) = 0$  has a positive root, that is,  $\det(L_n(c_2^{S_n})) = 0$ .

Define

$$M := \left\{ c_2^{S_n} : \det \left( L_n \left( c_2^{S_n} \right) \right) = 0, \quad 0 < c_2^{S_n} < z_2^+/z_1, n = 1, 2, \dots \right\}, \tag{3.3}$$

the set of all critical values for the parameter  $c_2$  for possible steady-state bifurcation. Then,  $M$  is non-empty under the aforementioned necessary condition as at least it contains  $c_2^{S_1}$ .

To check whether a  $c_2^{S_n} \in M$  is a true steady-state bifurcation point, one needs to verify the transversality condition. Note that  $M$  only has finitely many elements by virtue of the boundedness of  $p_{\pm}(c_2)$ . Let  $\lambda(c_2)$  be the solution of  $\Delta_n(\lambda) = 0$  satisfying  $\lambda(c_2^{S_n}) = 0$ . Then, we have the following transversality result.

**Lemma 3.3** *For fixed  $n \in \mathbb{N}$  and  $c_2^{S_n} \in M$ ,  $\text{Sign} \left\{ \frac{d}{dc_2} \lambda(c_2^{S_n}) \right\} = -\text{Sign} \left\{ \text{tr}(L_n)(c_2^{S_n}) \right\}$ , if  $\text{tr}(L_n)(c_2^{S_n}) \neq 0$ .*

*Proof* Taking the derivative of both sides of the equation  $\Delta_n(\lambda(c_2)) = 0$  with respect to  $c_2$ , and then replacing  $c_2$  by  $c_2^{S_n}$ , we obtain

$$\frac{d}{dc_2} \lambda \left( c_2^{S_n} \right) = \frac{1}{\text{tr}(L_n) \left( c_2^{S_n} \right)} \frac{d}{dc_2} \det(L_n) \left( c_2^{S_n} \right).$$

Noting that

$$\frac{d}{dc_2} \det(L_n)(c_2) < 0$$

for any fixed  $c_1 \in (0, z_1/z_2^+)$  and  $c_2 \in (0, z_2^+/z_1)$ , the proof is then completed.  $\square$

Now we are ready to state the main result on steady-state bifurcations.

**Theorem 3.4** *Given  $f, g, z_1, z_2^+, c_1$  and  $d < z_2^+ g'(z_2^+)$ , suppose that  $c_2^{S_k} \in M$  satisfies the following assumption:*

$$(H) \quad \text{tr}(L_k) \left( c_2^{S_k} \right) \neq 0 \text{ and } c_2^{S_k} \neq c_2^{S_n} \text{ for any } c_2^{S_n} \in M \text{ and } n \neq k.$$

*Then, there exists a smooth curve  $\Gamma_k$  of steady state of (1.6) bifurcating from  $(c_2, u, v) = (c_2^{S_k}, u^*, v^*)$ , with  $\Gamma_k$  contained in a global branch  $C_k$  of the nonzero steady states of (1.6). Moreover:*

- (i) *Near  $(c_2^{S_k}, u^*, v^*)$ ,  $\Gamma_k = \{(c_2(s), u(s), v(s)) : s \in (-\epsilon, \epsilon)\}$ , where  $u(s) = u^* + sa_k \cos(kx) + s\psi_1(s)$ ,  $v(s) = v^* + sb_k \cos(kx) + s\psi_2(s)$  for some smooth functions  $c_2(s)$ ,  $\psi_1(s)$  and  $\psi_2(s)$  such that  $c_2(0) = c_2^{S_k}$ ,  $\psi_1(0) = \psi_2(0) = 0$ ,  $\psi_1, \psi_2 \in \{\psi : \int_0^\pi \psi(x) \cos(kx) dx = 0\}$  and  $a_k, b_k$  satisfy  $L_k(c_2^{S_k})(a_k, b_k)^T = (0, 0)^T$ .*
- (ii)  *$C_k$  either contains another  $(c_2^{S_n}, u^*, v^*)$ ,  $c_2^{S_n} \in M$ ; or there exist  $c_2 \in (0, z_2^+/z_1)$  and  $v(x) \leq z_2^-/c_2$  such that  $(c_2, 0, v(x)) \in C_k$  or  $(c_2, z_1/c_1, 0) \in C_k$ ; or the projection of  $C_k$  onto  $c_2$ -axis contains the interval  $(c_2^{S_k}, z_2^+/z_1)$  or  $(0, c_2^{S_k})$ .*

The first statement is on local steady-state bifurcation. It follows directly from Lemma 3.3 and [26, Theorem 3.2]. Before moving to the proof for the second statement, we first recall the following maximum principle (see [26] and the references therein) and Harnack inequality (see [13] and the references therein).

**Lemma 3.5** *Let  $\Omega$  be a bounded Lipschitz domain in  $\mathbb{R}^n$ , and let  $g \in C(\bar{\Omega} \times \mathbb{R})$ . If  $z \in W^{1,2}(\Omega)$  is a weak solutions of the inequalities*

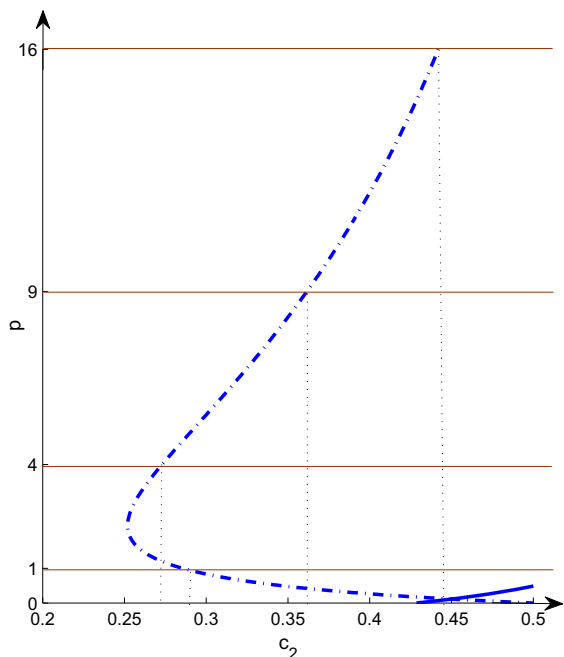


**Fig. 3** Graph of  $h(p) = 0$  and  $\text{tr}(L_p) = 0$  with  $z_1 = 2, z_2^+ = 1, c_1 = 1.5, f'(z_1) = -0.5$  and  $g'(z_2^+) = 0.5$ . The horizontal lines are  $p = n^2, n \in \mathbb{N}_0$

$$\Delta z + g(x, z) \geq 0 \text{ in } \Omega, \quad \partial z \leq 0 \text{ on } \partial\Omega,$$

and if there is a constant  $K$  such that  $g(x, z) < 0$  for  $z > K$ , then  $z \leq K$  a.e. in  $\Omega$ .

**Lemma 3.6** Let  $\Omega$  be a bounded Lipschitz domain in  $\mathbb{R}^n$ , and let  $c(x) \in L^q(\Omega)$  for some  $q > n/2$ . If  $z \in W^{1,2}(\Omega)$  is a weak solutions of the boundary value problem

$$\Delta z + c(x)z = 0 \text{ in } \Omega, \quad \partial z = 0 \text{ on } \partial\Omega,$$

then there is a constant  $C_1$ , determined only by  $\|c\|_q, q$  and  $\Omega$ , such that

$$\sup_{\Omega} z \leq C_1 \inf_{\Omega} z.$$

*Proof of Theorem 3.4 (ii)* Let  $(u(x), v(x))$  be a non-negative steady state solution of (1.6). Then, by Lemma 3.5, we have

$$0 \leq u(x) \leq z_1/c_1 \text{ and } 0 \leq v(x) \leq z_2^-/c_2, \text{ a.e. in } [0, \pi], \tag{3.4}$$

which then implies that

$$\|f(c_1 u(x) + v(x))\|_{L^\infty} \leq \max\{f(0), |f(z_1 + z_2^-/c_2)|\}$$

and

$$\begin{aligned} & \|g(u(x) + c_2 v(x))\|_{L^\infty} \\ & \leq \max \left\{ |g(0)|, |g(z_1/c_1 + z_2^-)|, \max_{z \in (z_2^+, z_2^-)} g(z) \right\}. \end{aligned}$$

By using the Harnack inequality in Lemma 3.6, we see that there exists a constant  $\tilde{C}$ , such that

$$\sup_{(0,\pi)} u(x) \leq \tilde{C} \inf_{(0,\pi)} u(x) \text{ and } \sup_{(0,\pi)} v(x) \leq \tilde{C} \inf_{(0,\pi)} v(x). \tag{3.5}$$

Next we claim that if  $(c_2, 0, v(x)) \notin \mathcal{C}_k$  and  $(c_2, z_1/c_1, 0) \notin \mathcal{C}_k$  for any  $c_2 \in (0, z_2^+/z_1), v(x) \in W^{1,2}[0, \pi]$  and  $v(x) \leq z_2^-/c_2$ , then all solutions in  $\mathcal{C}_k$  are bounded. Indeed, note that the solutions in  $\mathcal{C}_k$  near bifurcation point are positive. It then follows from (3.4) and (3.5) that we only need to prove that if  $(c_2, 0, v(x)) \notin \mathcal{C}_k$  and  $(c_2, z_1/c_1, 0) \notin \mathcal{C}_k$  for any  $c_2 \in (0, z_2^+/z_1), v(x) \in W^{1,2}[0, \pi]$  and  $v(x) \leq z_2^-/c_2$ , then there exists a constant  $K$  such that

$$\sup_{(0,\pi)} u > K \text{ and } \sup_{(0,\pi)} v > K, \text{ for } (c_2, u(x), v(x)) \in \mathcal{C}_k.$$

We argue by contradiction by assuming that this is not true. Then, there exists a sequence  $(c_2^n, u_n, v_n) \in \mathcal{C}$  such that  $\sup_{(0,\pi)} u_n(x) \rightarrow 0$  or  $\sup_{(0,\pi)} v_n(x) \rightarrow 0$  as  $n \rightarrow \infty$ . Consequently, there exists a subsequence, which we still denote by  $(c_2^n, u_n, v_n)$ , such that  $c_2^n \rightarrow c_2^\infty, u_n \rightarrow u_\infty$  and  $v_n \rightarrow v_\infty$  as  $n \rightarrow \infty$  with  $u_\infty = 0$  or  $v_\infty = 0$ . If  $v_\infty = 0$ , then  $u_\infty$  satisfying the following equation:

$$\Delta u_\infty + u_\infty f(c_1 u_\infty) = 0,$$

which only has two solutions 0 and  $z_1/c_1$  according to [7, Lemma 10.1.1]. It contradicts with  $(c_2, z_1/c_1, 0) \notin \mathcal{C}_k$ . Similarly, if  $u_\infty = 0$ , then  $v_\infty$  satisfies

$$\Delta v_\infty + v_\infty g(c_2 v_\infty) = 0,$$

contradicting with  $(c_2, 0, v) \notin \mathcal{C}_k$ . The proof is completed.  $\square$

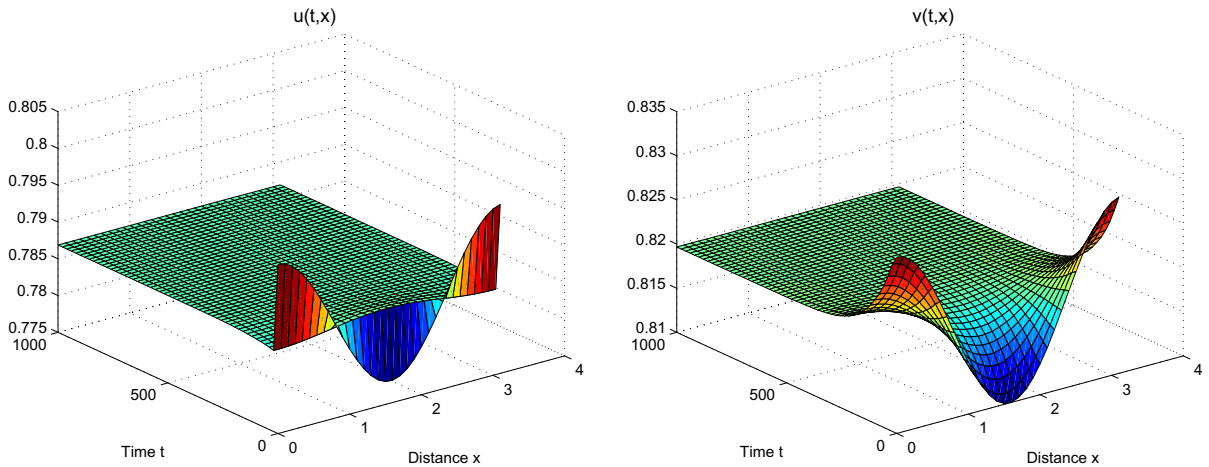


**Fig. 4** Numerical simulation for (1.6) with  $f(z) = 1 - z/2$ ,  $g(z) = -(x - 2)^2/4 + 1/4$ ,  $c_1 = 1.5$ ,  $d = 0.02$  and  $c_2 = 0.26$ . The initial functions are  $(0.78 + 0.01 \cos(2x), 0.82 + 0.01 \cos(2x))$ . The solution tends to a positive steady state

### 3.2 Hopf bifurcations

In this subsection, we still assume that  $d < z_2^+ g'(z_2^+)$  and explore possible Hopf bifurcation(s). Parallel to  $c_2^{S_n}$  in the preceding section, we define

$$c_2^{H_n} := \frac{-c_1 z_2^+ f'(z_1) + n^2(1 + d)}{(z_1 - c_1 z_2^+)g'(z_2^+) - c_1 z_1 f'(z_1) + c_1 n^2(1 + d)}, \quad n \in \mathbb{N}_0, \tag{3.6}$$

which is the solution of  $\text{tr}(L_n)(c_2) = 0$  and is a possible Hopf bifurcation point. The following lemma describes the basic properties of  $c_2^{H_n}$ .

**Lemma 3.7** *The following statement holds.*

- (i)  $0 < c_2^{H_0} < z_2^+ / z_1$ ;
- (ii)  $c_2^{H_m} < c_2^{H_n}$ , if  $m < n$ .

*Proof* (i) Since  $z_1 > c_1 z_2^+$  and  $g'(z_2^+) > 0$ , a direct calculation gives

$$c_2^{H_0} = \frac{-c_1 z_2^+ f'(z_1)}{(z_1 - c_1 z_2^+)g'(z_2^+) - c_1 z_1 f'(z_1)} < z_2^+ / z_1.$$

(ii) Consider the following function

$$\tilde{c}_2(p) = \frac{-c_1 z_2^+ f'(z_1) + p(1 + d)}{(z_1 - c_1 z_2^+)g'(z_2^+) - c_1 z_1 f'(z_1) + c_1 p(1 + d)}.$$

Differentiating it with respect to  $p$ , we obtain

$$\frac{d\tilde{c}_2(p)}{dp} = \frac{(1 + d)(z_1 - c_1 z_2^+)g'(z_2^+) - c_1 f'(z_1)(1 + d)(z_1 - c_1 z_2^+)}{[(z_1 - c_1 z_2^+)g'(z_2^+) - c_1 z_1 f'(z_1) + c_1 p(1 + d)]^2} > 0.$$

Therefore,  $\tilde{c}_2(p)$  is a strictly increasing function, proving (ii). □

Define

$$N := \left\{ c_2^{H_n} : 0 < c_2^{H_n} < z_2^+ / z_1 \text{ and } c_2^{H_n} < c_2^{S_n}, \text{ for } n \in \mathbb{N} \right\},$$

From Lemma 3.7, we know  $N \neq \emptyset$  and it indeed contains finitely many elements. The following lemma implies that  $N$  contains all possible Hopf bifurcation values for the parameter  $c_2$ .

**Lemma 3.8** *Given  $f, g, z_1, z_2^+$  and  $c_1$ ,  $\Delta_n(\lambda) = 0$  has a pair of purely imaginary solutions if and only if  $c_2 = c_2^{H_n} \in N$ .*

*Proof*  $\Delta_n(\lambda) = 0$  has a pair of purely imaginary solutions  $\lambda = \pm i\omega$  if and only if there exists  $n \in \mathbb{N}_0$  and  $\bar{c}_2$  such that

$$\text{tr}L_n(\bar{c}_2) = 0, \quad \det L_n(\bar{c}_2) > 0 \text{ and } \omega = \sqrt{\det L_n(\bar{c}_2)}.$$

From the definitions of  $c_2^{H_n}$ , we know that  $\text{tr}L_n(\bar{c}_2) = 0$  if and only if  $\bar{c}_2 = c_2^{H_n}$ . Next we examine  $\det L_n(c_2^{H_n}) > 0$  for  $c_2^{H_n} \in N$ . It is not difficult to calculate that  $\det L_n(c_2^{H_0}) > 0$  and  $\det L_n(c_2^{S_n}) = 0$ . For fixed  $n \in \mathbb{N}$ ,  $\det L_n(c_2)$  is a strictly decreasing function according to the proof of lemma 3.3. Thus, we obtain that  $\det L_n(c_2^{H_n}) > 0$  for  $c_2^{H_n} \in N$ . □

Let  $\lambda^H(c_2) = \gamma(c_2) + i\omega(c_2)$  be the root of  $\Delta_n(\lambda)$  satisfying  $\gamma(c_2^{H_n}) = 0$  and  $\omega(c_2^{H_n}) = \sqrt{\det L_n(c_2^{H_n})}$  for

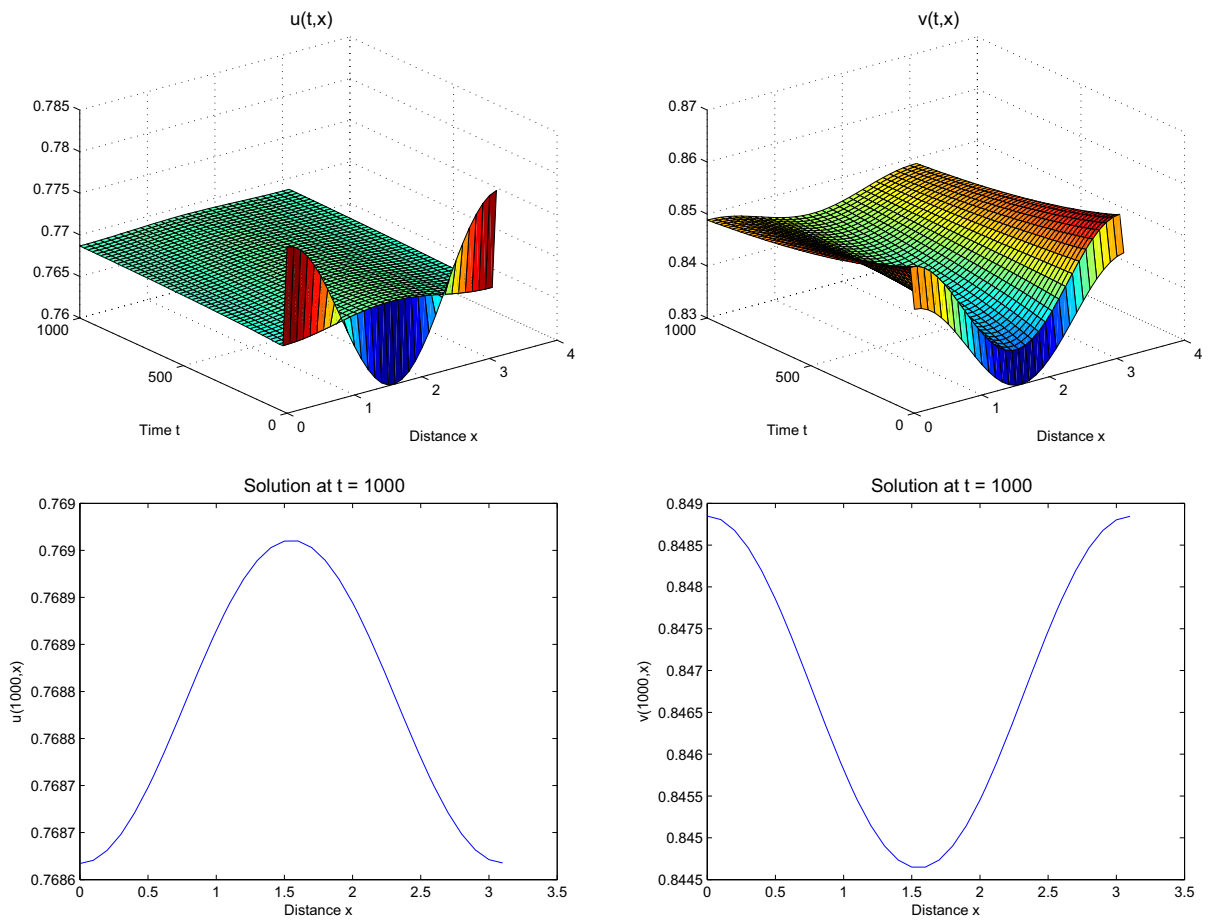


**Fig. 5** Numerical simulation for (1.6) with  $f(z) = 1 - z/2$ ,  $g(z) = -0.25(x - 2)^2 + 0.25$ ,  $c_1 = 1.5$ ,  $d = 0.02$  and  $c_2 = 0.273$ . The initial functions are  $(0.77+0.01 \cos(2x), 0.84+$

$0.01 \cos(2x))$ . The solution tends to a spatially inhomogeneous steady state which is a  $\cos(2x)$ -perturbation of the constant steady state

$c_2^{H_n} \in N$ . Then, we have the following transversality result.

**Lemma 3.9**  $\operatorname{Re} \left\{ \frac{d}{dc_2} \lambda^H(c_2^{H_n}) \right\} > 0$  for  $c_2^{H_n} \in N$ .

*Proof* Taking the derivative of both sides of the equation  $\Delta_n(\lambda^H(c_2)) = 0$  with respect to  $c_2$ , we have

$$\frac{d}{dc_2} \lambda^H(c_2) = \frac{\lambda(c_2) \frac{d \operatorname{tr} L_n(c_2)}{dc_2} - \frac{d \det L_n(c_2)}{dc_2}}{2\lambda(c_2) - \operatorname{tr} L_n(c_2)}.$$

Replacing  $c_2$  by  $c_2^{H_n}$  and separating real and imaginary parts, we have

$$\operatorname{Re} \left\{ \frac{d}{dc_2} \lambda^H(c_2^{H_n}) \right\} = \frac{1}{2} \frac{d}{dc_2} \operatorname{tr} L_n(c_2) = v^* g'(z_2^+) > 0$$

for any  $n \in \mathbb{N}_0$ . □

Based on the previous analysis on purely imaginary solutions of the characteristic equation as well as the Hopf bifurcation theorem, we immediately obtain the following result on Hopf bifurcations for (1.6).

**Theorem 3.10** For any  $c_2^{H_k} \in N$ , if  $c_2^{H_k} \neq c_2^{S_n}$  for any  $c_2^{S_n} \in M$  with  $n \neq k$ , then Hopf bifurcation occurs at  $c_2 = c_2^{H_k}$ .

*Remark 3.11* It is clear that the periodic solutions bifurcated from  $c_2 = c_2^{H_0}$  are spatially homogeneous, while those bifurcated from  $c_2^{H_n}$  with  $n \geq 1$  are spatially inhomogeneous. Moreover, by Lemmas 3.3, 3.9 and Ruan and Wei [16, Corolary 2.4] we know that all spatially inhomogeneous bifurcating periodic solutions are unstable, because there is an unstable manifold. We

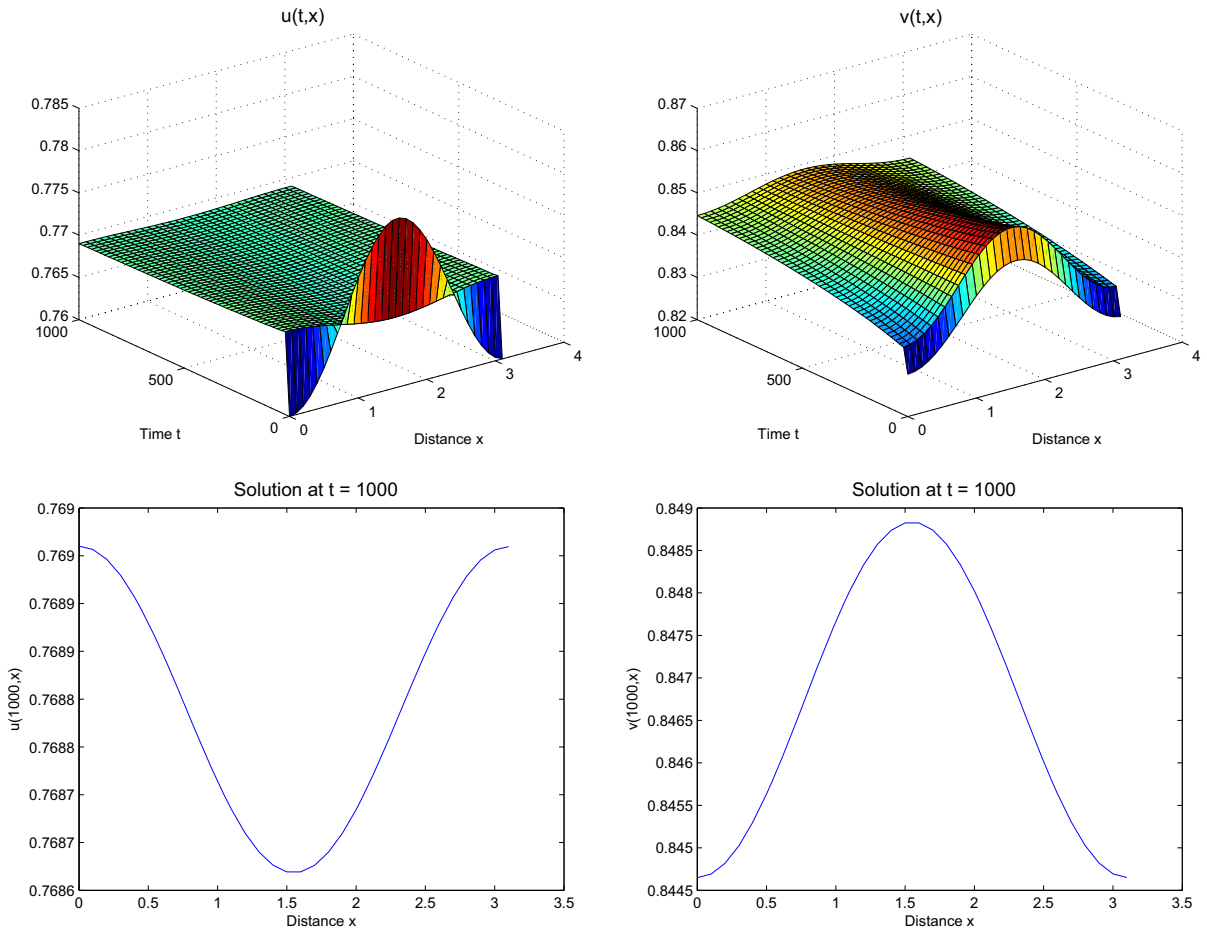


**Fig. 6** Numerical simulation for (1.6) with  $f(z) = 1 - z/2$ ,  $g(z) = -0.25(x - 2)^2 + 0.25$ ,  $c_1 = 1.5$ ,  $d = 0.02$  and  $c_2 = 0.273$ . The initial functions are  $(0.77 - 0.01 \cos(2x), 0.84 -$

$0.01 \cos(2x))$ . The solution tends to a spatially inhomogeneous steady state which is a  $\cos(2x)$ -perturbation of the constant steady state

also point out that the stability of the bifurcated periodic solutions on the center manifold can be determined by directly using the formula (2.31) in [26], but the formula is very lengthy for our model, and hence, we omit the details here.

Let  $c_2^* := \min\{c : c \in M \cup N\}$ . Combining our results obtained above with the result in Ruan and Wei [16, Corollary 2.4], we then obtain the following result on the stability of the positive steady state.

**Theorem 3.12** *The positive steady state  $(u^*, v^*)$  is asymptotically stable when  $c_2 \in (0, c_2^*)$  and unstable when  $c_2 > c_2^*$ .*

### 4 Numerical simulations and discussions

In this section we present some numerical simulations for (1.6) to illustrate and extend our analytic results. To this end, we need to choose particular functions for  $f$  and  $g$ . Theoretically, any  $f$  and  $g$  satisfying (1.2) and (1.3) can be used; biologically  $f$  and  $g$  can be specified based on the characteristics of the involving pioneer species and climax species. Here, our main purpose is to numerically demonstrate that a positive steady state can lose its stability either through Turing bifurcation or through Hopf bifurcation. For demonstration of the former (i.e., Turing bifurcation), we take the following relative simple functions for  $f(z)$  and  $g(z)$ :

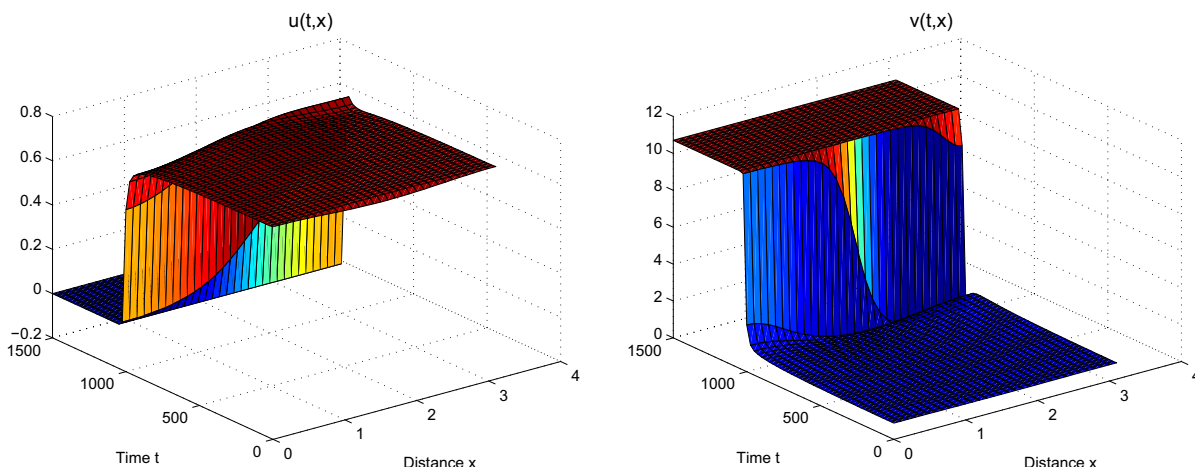


**Fig. 7** Numerical simulation for (1.6) with  $f(z) = 1 - z/2$ ,  $g(z) = -0.25(x - 2)^2 + 0.25$ ,  $c_1 = 1.5$ ,  $d = 0.02$  and  $c_2 = 0.28$ . The initial functions are  $(0.75 + 0.01 \cos(2x), 0.87 + 0.01 \cos(2x))$ . The solution converges to a boundary steady state

$$f(z) = 1 - z/2 \quad \text{and} \quad g(z) = -(z - 2)^2/4 + 1/4. \tag{4.1}$$

For these two functions, (1.2) and (1.3) obviously hold, with  $z_1 = 2$ ,  $z_2^+ = 1$  and  $z_2^- = 3$ . We choose  $c_1 = 1.5$  and  $d = 0.02$  so that

$$c_1 < z_1/z_2^+ = 2 \quad \text{and} \quad d < z_2^+ g'(z_2^+) = 0.5.$$

Then, we may numerically obtain all possible steady-state and Hopf bifurcation points for the parameter  $c_2$ , as indicated in Fig. 3, where the intersections of the parallel horizontal lines with the broken curve are the steady-state bifurcation points and the intersections of the parallel horizontal lines with the full curve are the Hopf bifurcation points. Therefore, in the interval of interest  $(0, z_2^+/z_1) = (0, 1/2)$  for  $c_2$ , there are four steady-state bifurcation points and one Hopf bifurcation point, and they have the following order:

$$0 < c_2^{S_2} \approx 0.2716 < c_2^{S_1} \approx 0.2853 < c_2^{S_3} \approx 0.3616 < c_2^{H_0} \approx 0.4286 < c_2^{S_4} \approx 0.4420 < z_2^+/z_1 = 0.5.$$

Thus,  $c_2^* = c_2^{S_2} \approx 0.2716$  according to the definition of  $c_2^*$ .

The numerical simulation given in Fig. 4 shows that a positive spatially homogeneous steady state exists and is asymptotically stable when  $c_2 < c_2^*$ . Figures 5 and 6 illustrate that when  $c_2$  passes through  $c_2^*$ , two stable spatially inhomogeneous steady states appear and they are  $\cos(2x)$ -perturbations of the constant steady state, suggesting that  $c_2^*$  is a actually pitchfork bifurcation

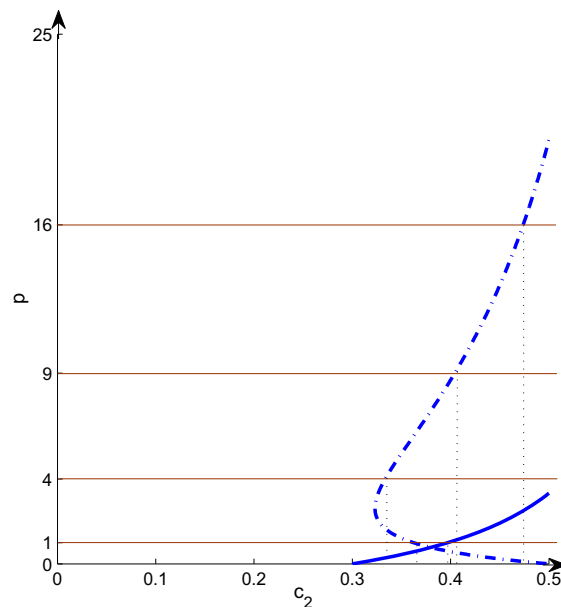


**Fig. 8** Graph of  $h(p) = 0$  and  $\text{tr}(L_p) = 0$  with  $z_1 = 2$ ,  $z_2^+ = 1$ ,  $c_1 = 1.5$ ,  $d = 0.2$ ,  $f'(z_1) = -1$  and  $g'(z_2^+) = 4$ . The horizontal lines are  $p = n^2$ ,  $n \in \mathbb{N}_0$

point (see also [19] for a similar result). On the other hand, it has been shown in [3] that the constant steady state is stable under homogeneous perturbations when  $c_2 < c_2^{H_0}$ . Therefore, Turing instability occurs when  $c_2$  passes through  $c_2^*$  but remains in  $(c_2^*, c_2^{H_0})$  since  $c_2^* < c_2^{H_0}$ .

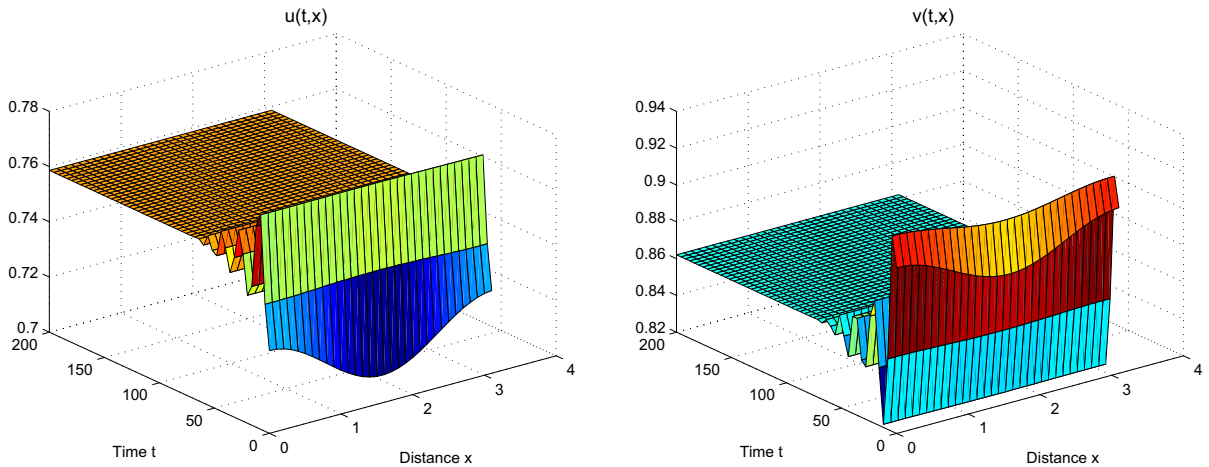


**Fig. 9** Numerical simulation for (1.6) with  $f(z) = 2 - z$ ,  $g(z) = -4(x - 2)^2 + 4$ ,  $c_1 = 1.5$ ,  $d = 0.2$  and  $c_2 = 0.28$ . The initial functions are  $(0.72 + 0.01 \cos(2x), 0.9 + 0.01 \cos(2x))$ . The solution approaches a uniformly positive steady state

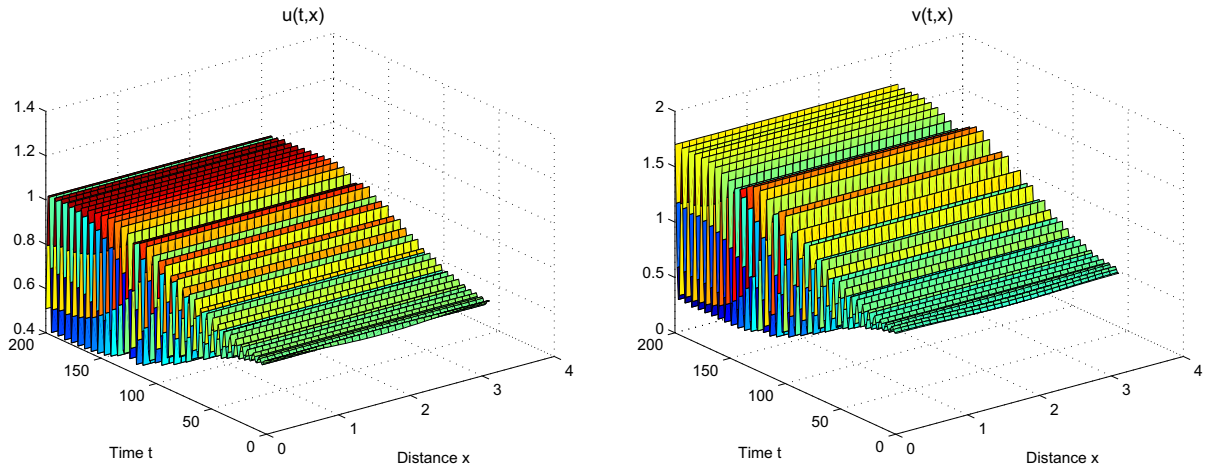


**Fig. 10** Numerical simulation for (1.6) with  $f(z) = 2 - z$ ,  $g(z) = -4(x - 2)^2 + 4$ ,  $c_1 = 1.5$ ,  $d = 0.2$  and  $c_2 = 0.305$ . The initial functions are  $(0.72 + 0.01 \cos(2x), 0.9 + 0.01 \cos(2x))$ . The solution tends to a uniformly positive steady state

In Fig. 7, we increase  $c_2$  a little bit to  $0.28 \in (c_2^{S_2}, c_2^{S_1})$  and choose a  $\cos(2x)$ -perturbation of the constant coexistence steady state as the initial function. We see that the solution converges to the boundary steady state  $(0, z_2^-/c_2)$ . Combining this numerical observation and the global steady-state bifurcation Theorem 3.4 (ii), we may expect that the bifurcation branch bifurcated from  $c_2^{S_2}$  contains the boundary steady state  $(0, z_2^-/c_2)$ . As such, as  $c_2$  increases, the constant coexistence steady state loses its stability and the bifurcated stable spatially inhomogeneous coexistence steady state evolves and merges into the boundary constant steady state  $(0, z_2^-/c_2)$ . This means

that the climax species becomes dominant as  $c_2$  passes through  $c_2^*$ .

To observe the scenario that the positive steady state loses its stability through Hopf bifurcation, we choose

$$f(z) = 2 - z \quad \text{and} \quad g(z) = -4(z - 2)^2 + 4. \quad (4.2)$$

Then, direct calculations yield

$$z_1 = 2, \quad z_2^+ = 1, \quad z_2^- = 3.$$

Set  $c_1 = 1.5$  and  $d = 0.2$  so that

$$c_1 < z_1/z_2^+ = 2 \quad \text{and} \quad d < z_2^+ g'(z_2^+) = 0.5.$$

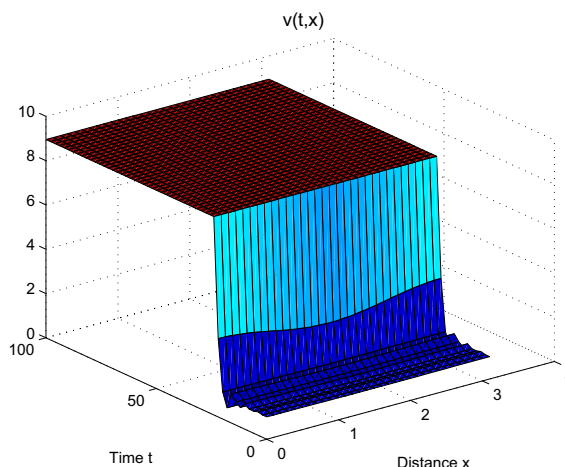
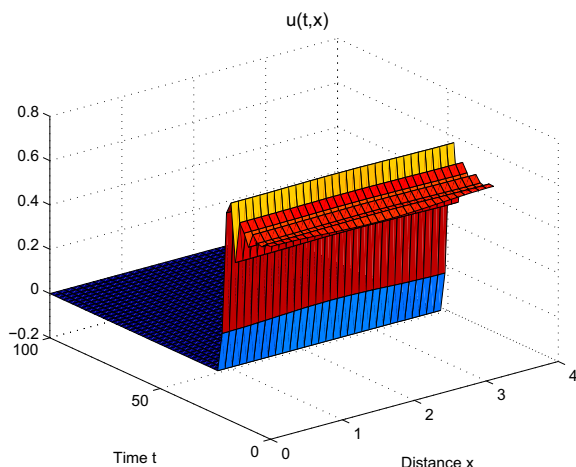


**Fig. 11** Numerical simulation for (1.6) with  $f(z) = 2 - z$ ,  $g(z) = -4(x - 2)^2 + 4$ ,  $c_1 = 1.5$ ,  $d = 0.2$  and  $c_2 = 0.335$ . The initial functions are  $(0.66 + 0.01 \cos(2x), 1 + 0.01 \cos(2x))$ .

The solution oscillates in the very beginning and then tends to a boundary steady state

With the above choice, the numerical result given in Fig. 8 depicts all steady-state and Hopf bifurcation points for  $c_2 \in (0, z_2^+/z_1)$ , with the intersections of the parallel horizontal lines with the broken curve being the steady-state bifurcation points and the intersections of the parallel horizontal lines and the full curve being the Hopf bifurcation points. As is seen in Fig. 8, there are four steady-state bifurcation points and two Hopf bifurcation points, and they have the following order:

$$0 < c_2^{H_0} = 0.3 < c_2^{S_2} \approx 0.3334 < c_2^{S_1} \approx 0.3632 < c_2^{H_1} \approx 0.3968 < c_2^{S_3} \approx 0.4152 < c_2^{S_4} \approx 0.4712 < z_2^+/z_1 = 0.5.$$

Therefore,  $c_2^* = c_2^{H_0} = 0.3$ . Figure 9 shows that the positive spatially homogeneous steady state is asymptotically stable when  $c_2 < c_2^*$ . Note that  $c_2^*$  is the first Hopf bifurcation point of the spatially homogeneous equation (1.4). It then follows that no Turing bifurcation occurs in such a case. As  $c_2$  passes through  $c_2^*$ , but stay in  $(c_2^*, c_2^{S_2})$ , no Turing bifurcation occurs and the bifurcated spatially homogeneous time periodic solution is asymptotically stable (see Fig. 10).

Finally, we choose  $c_2$  to be further away from the first Hopf bifurcation point  $c_2^{H_0}$  and numerically find that the bifurcated time periodic solutions disappear and the solution starting from a  $\cos(2x)$ -perturbation of the positive steady state converges to the boundary steady state  $(0, z_2^-/c_2)$ . This again indicates that the

climax species becomes dominate as  $c_2$  is away from  $c_2^*$  (Fig. 11).

### 5 Conclusions

We have analyzed the diffusive pioneer–climax interaction model (1.6) with the no-flux boundary condition. We have found that the diffusion does not affect the stability/instability of boundary equilibria, neither does the diffusion change the instability of the unstable coexistence equilibria. But the diffusion can destroy the stability of those stable coexistence equilibria, and the consequence of the loss of stability of such a coexistence equilibrium can be either Turing bifurcation leading to pattern formation or Hopf bifurcation leading to a temporally periodic solution. Conditions for each of the two cases are obtained, and are numerically demonstrated by choosing some particular functions for the two interaction terms  $f$  and  $g$ .

Note that the functions given in (4.1) and (4.2) for  $f$  and  $g$  are of the same type. Indeed, the  $f$  in (4.1) is nothing but just the half of the  $f$  given in (4.2), while the  $g$  in (4.1) is the sixteenth of the  $g$  given in (4.2). However, as was seen in Sect. 4, such a small difference can lead to significant difference in bifurcation paths as  $c_2$  is increased. These two numerical examples indicate that really the particular forms of functions  $f$  and  $g$  and the involving parameters matter a lot. Of course, when

applying the model (1.6) to a particular pair of pioneer and climax species, we need to choose  $f$  and  $g$  to reflect the main biological feature of these two species, as in [1, 15, 23]. There are also some discussions on this topic in [17] where the corresponding ODE version (1.1) was initially proposed.

In this paper, we have used  $c_2$  as the bifurcation parameter, which reflects the relative weight of the impact of the *intra-species interaction* versus that of the *inter-species interaction* on the climax species  $v$ . Thus, small  $c_2$  would correspond to a scenario of *inter-species interaction dominance*, while large  $c_2$  would explain an scenario of *intra-species interaction dominance*. This together with the other conditions on diffusion rates (large  $d := d_2/d_1$ ) in Sect. 3 and the nature of the per capita growth function  $g$  for species  $v$  explains, to certain extent, why increasing  $c_2$  (under appropriate conditions on  $d$ ) would destroy the stability of a stable positive (coexistence) equilibrium. As explained above, the bifurcation path is sensitive to the particular pair of  $f$  and  $g$ . Moreover, our simulation results in Sect. 4 show that the bifurcations at  $c_2^*$  are supercritical. We point out that for general case, determination of the direction of bifurcation and the stability of the bifurcated spatial–temporal dynamics requires very dedicate and lengthy computations of normal form and central manifold, and is thus omitted in this paper.

## References

1. Allee, W.C.: *Animal Aggregations: A Study in General Sociology*. University of Chicago Press, Chicago (1931)
2. Brown, S., Dockery, J., Pernarowski, M.: Traveling wave solutions of a reaction diffusion model for competing pioneer and climax species. *Math. Biosci.* **194**, 21–36 (2005)
3. Buchanan, J.R.: Asymptotic behavior of two interacting pioneer/climax species. *Fields Inst. Commun.* **21**, 51–63 (1999)
4. Buchanan, J.R.: Turing instability in pioneer/climax species interactions. *Math. Biosci.* **194**, 199–216 (2005)
5. Cantrell, R.S., Cosner, C.: *Spatial Ecology via Reaction–Diffusion Equations*, Wiley Series in Mathematical and Computational Biology. Wiley, Chichester (2003)
6. Dockery, J., Hutson, V., Mischaikow, K., Pernarowski, M.: The evolution of slow dispersal rates: a reaction–diffusion model. *J. Math. Biol.* **37**, 61–83 (1998)
7. Henry, D.: *Geometric Theory of Semilinear Parabolic Equations*. Lecture Notes in Mathematics, vol. 840. Springer, Berlin (1981)
8. Jin, J., Shi, J., Wei, J., Yi, F.: Bifurcations of patterned solutions in the diffusive Lengyel–Epstein system of CIMA chemical reactions. *Rocky Mt. J. Math.* **43**, 1637–1674 (2013)
9. Li, X., Jiang, W., Shi, J.: Hopf bifurcation and Turing instability in the reaction–diffusion Holling–Tanner predator–prey model. *IMA J. Appl. Math.* **78**, 287–300 (2013)
10. Liu, J., Wei, J.: Bifurcation analysis of a diffusive model of pioneer and climax species interaction. *Adv. Differ. Equ.* **52**, 1–11 (2011)
11. Mizoguchi, N., Ninomiya, H., Yanagida, E.: Diffusion-induced blowup in a nonlinear parabolic system. *J. Dyn. Differ. Equ.* **4**, 619–638 (1998)
12. Pao, C.V.: *Nonlinear Parabolic and Elliptic Equations*. Plenum, New York (1992)
13. Peng, R., Shi, J., Wang, M.: On stationary patterns of a reaction–diffusion model with autocatalysis and saturation law. *Nonlinearity* **21**, 1471–1488 (2008)
14. Peng, R., Yi, F., Zhao, X.: Spatiotemporal patterns in a reaction–diffusion model with the Degrn–Harrison reaction scheme. *J. Differ. Equ.* **254**, 2465–2498 (2013)
15. Ricker, W.E.: Stock and recruitment. *J. Fish. Res. Board Can.* **11**, 559–623 (1954)
16. Ruan, S., Wei, J.: On the zeros of transcendental functions with applications to stability of delay differential equations with two delays. *Dyn. Contin. Discrete Impuls. Syst. Ser. A Math. Anal.* **10**, 863–874 (2003)
17. Selgrade, J.F., Namkoong, G.: Stable periodic behavior in a pioneer-climax model. *Nat. Resour. Model.* **4**, 215 (1990)
18. Selgrade, J.F., Roberds, J.H.: Lumped-density population models of pioneer-climax type and stability analysis of Hopf bifurcations. *Math. Biosci.* **135**, 1–21 (1996)
19. Song, Y., Zou, X.: Bifurcation analysis of a diffusive ratio-dependent predator–prey model. *Nonlinear Dyn.* **78**, 49–70 (2014)
20. Su, Y., Zou, X.: Transient oscillatory patterns in the diffusive non-local blowfly equation with delay under the zero-flux boundary condition. *Nonlinearity* **27**, 87–104 (2014)
21. Sumner, S.: Competing species models for pioneer-climax forest dynamical systems. *Proc. Dyn. Syst.* **1**, 351–358 (1994)
22. Turing, A.M.: The chemical basis of morphogenesis. *Phil. Trans. R. Soc. Lond. B* **237**, 37–72 (1952)
23. Verhulst, P.F.: Notice sur la loi que la population poursuit dans son accroissement. *Corresp. Math. Phys.* **10**, 113–121 (1838)
24. Wang, J., Wei, J., Shi, J.: Global bifurcation analysis and pattern formation in homogeneous diffusive predator–prey systems. *J. Differ. Equ.* **260**, 3495–3523 (2016)
25. Weng, P., Zou, X.: Minimal wave speed and spread speed of competing pioneer and climax species. *Appl. Anal.* **93**, 2093–2110 (2014)
26. Yi, F., Wei, J., Shi, J.: Bifurcation and spatiotemporal patterns in a homogeneous diffusive predator–prey system. *J. Differ. Equ.* **246**, 1944–1977 (2009)
27. Yuan, Z., Zou, X.: Co-invasion waves in a reaction diffusion model for competing pioneer and climax species. *Nonlinear Anal. RWA* **11**, 232–245 (2010)
28. Zhou, J., Shi, J.: Pattern formation in a general glycolysis reaction diffusion system. *IMA J. Appl. Math.* **80**, 1703–1738 (2015)
29. Zuo, W., Wei, J.: Multiple bifurcations and spatiotemporal patterns for a coupled two-cell Brusselator model. *Dyn. Partial Differ. Equ.* **8**, 363–384 (2011)